

Morphological and biomechanical remodelling of the hepatic artery in a swine model of portal hypertension

Xi-Ju He · Ming-Hua Yu · Wen-Chun Li ·
Han-Qin Wang · Jing Li · Xing-Chun Peng ·
Jie Tang · Na Feng · Tie-Zhu Huang

Received: 21 October 2010 / Accepted: 18 July 2011 / Published online: 23 September 2011
© Asian Pacific Association for the Study of the Liver 2011

Abstract

Objectives To obtain the biomechanical and morphological remodelling of hepatic arteries in swine with portal hypertension.

Methods A number of 20 white pigs was used, of which 14 were subjected to liver cirrhosis and portal hypertension (PHT) induced by carbon tetrachloride and pentobarbital; the rest were used as the control group. The biomechanical remodelling of the hepatic arteries was measured, namely, the incremental elastic modulus (E_{inc}), pressure–strain elastic modulus (E_p), volume elastic modulus (E_v), the incremental compliance (C), the opening angle and the stained microstructural components of the vessels.

Results The percentages for the microstructural components and the histologic data significantly changed in the experimental group, three incremental elastic moduli (E_{inc} , E_p , and E_v) of the experimental group were significantly larger than those of the control group ($P < 0.05$); the compliance of hepatic arteries decreased greatly ($P < 0.05$) too. The opening angle (OA) was considerably larger than that of control group ($P < 0.05$).

Conclusions The study suggests that the morphological and biomechanical properties of swine hepatic arteries have changed significantly during the process of portal hypertension and that from biomechanical aspects, the hepatic arteries have also suffered from extensive

remodelling, which in turn deteriorates the existing portal hypertension.

Keywords Portal hypertension · Hepatic artery · Hepatic artery buffer response · Remodelling · Elastic modulus · Compliance · Zero-stress state

Introduction

Liver is well known as a double blood-supply structure, with 75% of its total flow coming from the portal veins and the other 25% from the hepatic arteries [1, 2]. The blood flow of portal veins varies greatly in response to a wide variety of stimuli. Alterations of portal venous blood flow are countered by flow changes of the hepatic artery under physiological condition, aiming at maintaining the total hepatic blood flow [3, 4]. This mechanism described as the hepatic artery buffer response (HABR) seems to be regulated by adenosine [5, 6]. And the responsible receptor for adenosine-mediated vasodilatation in the hepatic artery of normal livers is the adenosine A_2 receptor [7]. Several researchers have investigated this response and found that nitric oxide (NO) and H_2S are also responsible for HABR [8–11].

During the process of portal hypertension (PHT), the altered haemodynamics crucially deteriorates tissue oxygenation and liver function, which may cause hypoxaemia in cirrhosis and the HABR shown in others' previous studies [12, 13]. Due to the existence of HABR, the hepatic arterial blood flow becomes more and more significant during the development of PHT. In fact, vascular remodelling has been shown in pulmonary and superior mesenteric arteries of cirrhotic animals [14, 15].

To the best of our knowledge, major interest of the previous studies has been focused on vasoactive substances

X.-J. He · M.-H. Yu · W.-C. Li · H.-Q. Wang · J. Li ·
X.-C. Peng · J. Tang · N. Feng · T.-Z. Huang (✉)
Institute of Basic Medical Sciences,
Hubei University of Medicine, Shiyan, China
e-mail: huizi630@yahoo.cn

M.-H. Yu
Department of Medical Oncology, Taihe Hospital,
Hubei University of Medicine, Shiyan, China

about HABR under physiological conditions [5, 7, 10], and only very few studies have addressed the role of HABR and the biomechanical remodelling of the hepatic artery under pathophysiological conditions. Zipprich [16] and his colleagues have investigated the response of adenosine in hepatic arteries of CCl₄-cirrhosis livers mediated mainly by the adenosine A₁ receptor. Both the CCl₄- and BDL-cirrhotic models have shown vascular remodelling in the intrahepatic arteries [17], but there are no existing data on extrahepatic vascular remodelling of hepatic arteries of PHT. Consequently, our study intends to establish a reliable swine CCl₄-cirrhotic PHT model in order to investigate the biomechanical and morphological remodelling of the extrahepatic vascular of hepatic arteries and provide some references for probing HABR and the in-depth pathogenesis of PHT and offer approaches to prevention and treatment of PHT.

Materials and methods

Establishment of swine PHT model

A number of 8 male and 12 female with 2-month-old healthy swine were applied with an initial average body weight of 16.5 kg and the study is performed in compliance with the state guidelines confirmed by institutional ethical committee for humane treatment and care of the laboratory animals. No obvious abnormality was found in liver function test and colour doppler ultrasonography (GE Medical Systems, Milwaukee, WI, USA) among the 20 pigs before the experiment. After 1 week of acclimation, 14 animals were administered carbon tetrachloride (CCl₄, Sigma) at a dose of 3 mg/kg/d after pretreatment with oral phenobarbitone (3 mg/kg/d) to induce liver cirrhosis and PHT [18, 19]. In order to accelerate this process and mimic the pathophysiological disturbances of PHT addressed in human studies, the experimental animals were subjected to continuous consumption of a diet containing 20% grease and 10% alcohol as the only drink. The treatment lasted for approximately 16 weeks. At the same time, the rest six swine of the same age and size were maintained with normal drinking water and swine chow and served as the control group.

Portal pressure determination and portal vein sampling

After measuring the body weight for the last time, swine of the two groups were anaesthetized with intramuscular injection of pentobarbital sodium (10 mg/kg) and ketamine (20 mg/kg). The anesthesia was maintained by cannulation of an ear vein and intravenous administration of additional pentobarbital sodium (2 mg/kg) and ketamine (2 mg/kg) until the end of the operation. The swine were placed in a

supine position with a midline incision in the abdominal wall and the portal vein exposed. A 5-Fr flow-directed thermodilution fiberoptic catheter (CCOmbio 744H5F, Edwards Swan-Ganz, Baxter Edwards Critical Care, Irvine, Calif, USA) filled with heparinized saline was inserted in the main portal vein from a distal puncture in the inferior mesenteric vein. The portal pressure was recorded via the catheter in the portal vein and connected to blood pressure transducers (Transpac Disposable Transducer, Abbott, Chicago, Ill, USA). During surgery, the body temperature of the animals was kept at $38 \pm 1^\circ\text{C}$ using an operating table heater and warmed fluids. When all surgical procedures were completed, the animals were killed with an overdose of pentobarbital sodium. The liver including the portal vein, the hepatic artery and the bile duct was rapidly removed together with the spleen and all were then placed in the physiological salt solution. The hepatic artery was gently dissected free from surrounding tissue and isolated carefully without any traction or protraction. The end close to the origin from the celiac artery was assigned as the proximal end, the opposite end close to its branching before entering the liver as the distal end.

Staining and image quantitative analysis

Before the distension test, the distal end of each blood vessel sample was quickly sliced up into 5- to 10- μm frozen transverse sections with a cold incubator microtome. The sections were stained with haematoxylin–eosin (HE), orange G, Weigert's iron–haematoxylin and aniline blue, respectively, then washed in tap water for 5 min at room temperature, dehydrated in ethanol/water series (30 s each) followed by three changes in absolute ethanol (2 min each) and cleared in xylene. The diameter, thickness and the microstructure components including smooth muscle (including the cellular nuclear number density, CNND and the cellular nuclear area density, CNAD), collagen and elastin of each blood vessel sample were measured and quantified by a computer image analysis system (Leica-Q500IW; Leica Ltd, Cambridge, UK). This system detected all pixels in the image that were equivalent to, or nearly equivalent to, the colour levels of the select area. The total area of each component was the sum of the areas covered by the fibre in the same field and was expressed as the percentage of the total area of the vessel wall [the relative content (Aa%)]. For each sample, readings were taken from six representative fields and the mean values obtained were used for analysis.

Biomechanical test

The pressure–diameter experiments were carried out as described previously [20, 21]. Before the pressure–diameter experiment, a small section of both ends was cut and

reserved in the Kreb's solution for opening angle (OA) experiments and the proximal and distal ends of the hepatic artery were fixed on a self-developed soft tissue mechanical test machine (supervised and produced by the Centre of Technology, Dongfeng Automobile Co., Ltd, Shiyang, China). The proximal end was connected to an electronic peristaltic pump and a pressure transducer through a three-way apparatus and the distal end was closed and fixed. The middle superior part of vessel was stained into a black band with the width of approximately 3 mm by using the oil-soluble black pigment. The samples were axially stretched to the length as in vivo; the pressure sensor was calibrated to zero before the test. The whole experiment was performed in a controlled temperature saline solution bath of $37 \pm 0.5^\circ\text{C}$. The vessel was preconditioned ten times with a step distension test. During the test, the Kreb's solution was infused into the vessels at a constant rate of 1.5 ml/min with the electronic peristaltic pump; the pressure was controlled at the range of 0–27 kPa with the increment of 3.0 kPa in each step. A camera was fixed above the vessel and focused on the black bands to monitor the changes of vascular diameter (D) with the alteration of pressure (P). The sampling rate was 100 times per min. After the pre-conditioning test, the step test was repeated five times as the final tests. The outer diameters of vessels were recorded at each pressure step.

Zero-stress state observation

After its ventral side was marked, the section reserved for OA experiment was cut into nearly 1-mm-long ring and was then placed in the Kreb's solution. After a radial cut was made in the ring along the coloured marking, the vessel ring sprang open rapidly and continued to open more slowly until it reached a constant OA for 20–30 min for the occurrence of viscoelastic creep. Photographs were taken by the camera connected to a computer, and signals were input to the computer and analysed (the angle between the two lines joining the midpoint of the inner arc of the cross-section to its tips was known as the opening angle).

Biomechanical analysis

As for the incremental Young's elastic modulus for cylinders extended by pressure at axial isometry having been relatively thin but not negligible thick walls the modulus defined by the classical work of Cox [22] is usually applied. Elastic modulus plotted against tensile stress is advised to characterize elasticity of wall material [23]. In this study, based on the pressure–diameter curves, the effective (isotropic) incremental Young's modulus (E_{inc}), the circumferential incremental modulus (E_v), the longitudinal incremental modulus (E_p) and the segment incremental compliance (C) were calculated as follows:

$$E_{inc} = 0.75 \cdot \Delta P / \Delta R \cdot R^2 / h$$

$$E_v = \Delta P / \Delta R \cdot R / 2$$

$$E_p = \Delta P / \Delta R \cdot R$$

$$C = dV/dP = 2\pi R \cdot \Delta R / \Delta P$$

While P , R , and h are pressure, radius and thickness of the blood vessel, respectively, ΔP is the pressure change and ΔR is the radius change.

Statistical analysis

Data were presented as means \pm SEM and differences between the groups were compared by t test. The statistical analysis was performed with SPSS 11.0 software (SPSS Co., Chicago, IL, USA). A value of $P < 0.05$ was considered statistically significant.

Results

At the end of 16th week, two swine of the experimental group died from acute serious hepatitis and upper gastrointestinal hemorrhage. The body weight of experimental group was 32.5 ± 2.1 kg ($n = 12$), lower than that of the control group (77.3 ± 3.6 kg, $P < 0.01$). Cirrhosis was histologically confirmed in CCl₄-cirrhotic animals and ascites were shown in all cirrhotic animals. The mean portal pressure of these swine (4.17 ± 1.03 kPa) was approximately threefold greater than that of the controls (1.51 ± 0.39 kPa, $P < 0.001$).

Portal hypertension leads to morphological and microstructural changes of hepatic artery

Using specific staining method, the morphological data and microstructural components have been demonstrated in Fig. 1. Figure 1(a–d) illustrates that hepatic artery is a muscular artery typically composed of three layers: the intima, the media and the adventitia. Internal elastic membrane is dense and wavy, which can be the result of fixation at zero pressure; the media membrane constitutes the majority of the hepatic artery wall and composed of the 10–20 lines of shuttle-shaped smooth muscle cells; between the smooth muscle cells there was a small amount of collagen fibers and elastic fibers, and matrix, the adventitia membrane was composed of loose connective tissue. Figure 1(e–h) illustrates that when portal hypertension, internal elastic membrane was ruptured or completely disappeared, elastic fibres were degraded and broken in media membrane (Fig. 1f), the cellular nuclear of smooth muscle cells were deformed and separated by

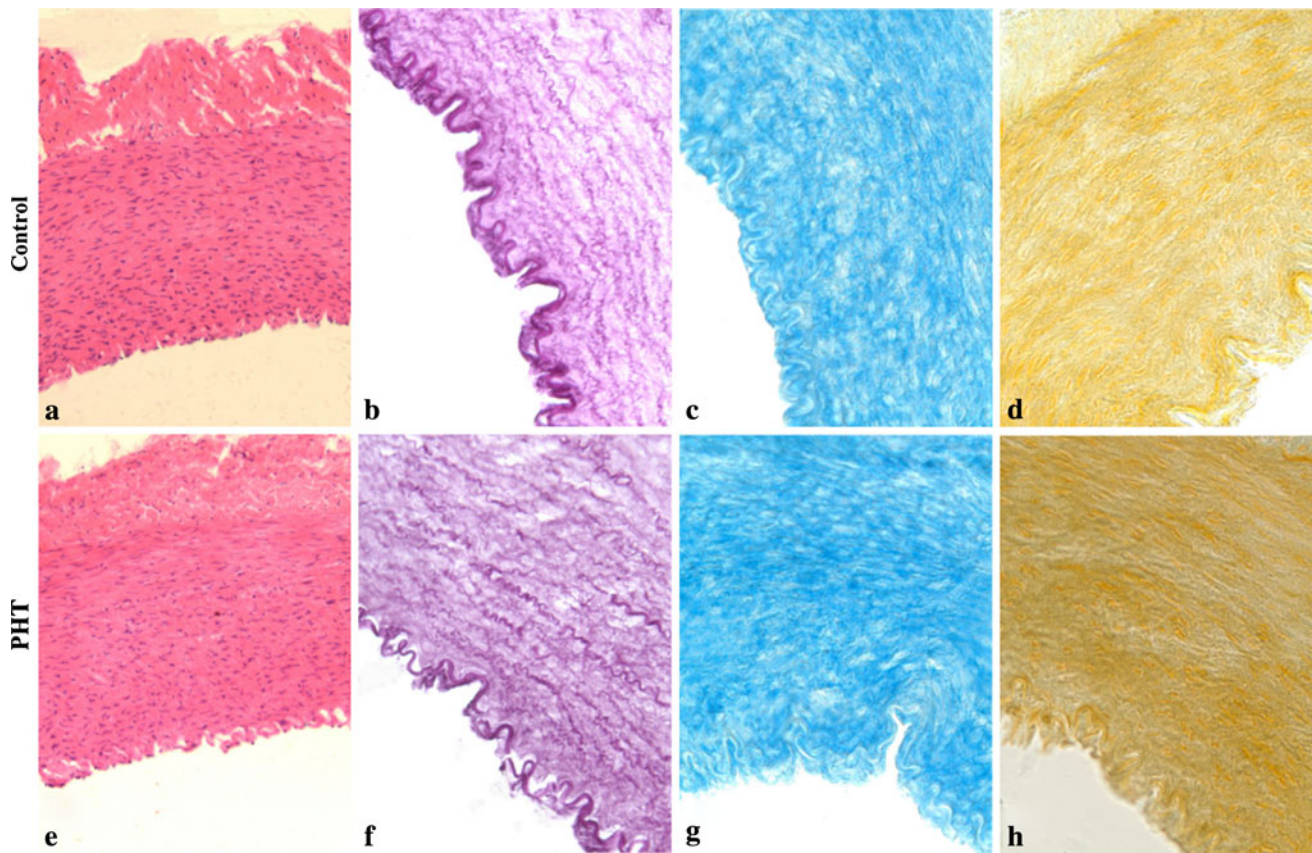


Fig. 1 The representative microstructure photographs of hepatic artery normal (*top panel*) and PHT (*lower panel*) swine

collagen fibres (Fig. 1e); collagen and extracellular matrix were increased in the entire wall (Fig. 1g).

Haematoxylin–eosin staining (a, e $\times 200$) was used to determine the vessel diameter, wall thickness, the CNND and the CNAD of smooth muscle cells; Weigert's iron–haematoxylin (b, f $\times 400$), Aniline Blue (c, g $\times 400$) and Orange G (d, h $\times 400$) specific staining were used to determine the relative content (Aa%) of the elastic fibers, collagen and smooth muscle in each vessel wall.

Quantified by a computer image analysis system, the histological data of the hepatic artery are shown in Table 1; while portal hypertension, the intima and media thickness and the diameter of hepatic artery were significantly higher than the control ($P < 0.05$), the wall thickness of hepatic artery is significantly higher than the control ($P < 0.01$).

The percentage of the microstructural components of the hepatic artery is shown in Table 2. When in the condition of portal hypertension, the percentage of collagen fibers of hepatic artery was significantly higher than the control ($P < 0.01$), the relative percentage of elastic fiber content decreased significantly ($P < 0.05$), with no significant changes in the percentages of smooth muscle; the ratio of C and E was significantly increased ($P < 0.01$), and the CNND and CNAD were also significantly increased ($P < 0.05$).

Portal hypertension induces biomechanical changes in hepatic artery wall

Based on the pressure–diameter curves, the lumen diameter (LD) and the media thickness (MT) of hepatic arteries from two groups were calculated and plotted against pressure (P). Figure 2 illustrates the relationship between LD (Fig. 2a), MT (Fig. 2b), and pressure (P), respectively. It indicates that the LD of hepatic artery in both groups increased with the pressure within the pressure range of 0 ~ 27 kPa, and the MT of hepatic artery of both groups decreased with the pressure. But at the same pressure, the LD and MT of hepatic artery of the PHT group were significantly higher than those of the control group ($P < 0.05$).

Based on the pressure–diameter curves, the effective (isotropic) incremental Young's modulus (E_{inc}), the circumferential incremental modulus (E_v), and the longitudinal incremental modulus (E_p) of hepatic arteries from two groups were calculated and plotted against pressures. Figure 3 illustrates the relationship between E_p (Fig. 3a), E_{inc} (Fig. 3b), E_v (Fig. 3c), and pressure, respectively. It indicates that within the pressure range of 0 ~ 27 kPa, three kinds of incremental elastic modulus of both groups

Table 1 Changes of the geometrical morphology of hepatic artery (Means ± SEM, mm)

	Control group (n = 6)	Experimental group (n = 12)
Intima thickness	0.033 ± 0.007	0.061 ± 0.008 ^b
Media thickness	0.198 ± 0.012	0.261 ± 0.017 ^a
Adventitia thickness	0.085 ± 0.010	0.087 ± 0.006
Wall thickness	0.313 ± 0.011	0.408 ± 0.012 ^b
Diameter	2.76 ± 0.315	3.541 ± 0.219 ^a

^a *P* < 0.05

^b *P* < 0.01, versus control group

Table 2 Changes of the microstructural components of hepatic artery (Mean ± SEM) %

	Control group (n = 6)	Experimental group (n = 12)
Collagen (Aa%)	10.47 ± 0.42	16.36 ± 0.71 ^b
Elastin (Aa%)	21.29 ± 1.65	15.92 ± 0.94 ^a
C/E	0.49 ± 0.09	0.96 ± 0.11 ^b
Smooth muscle (Aa%)	24.95 ± 1.36	29.24 ± 1.99
CNND (entries/mm ²)	5,149.68 ± 487.72	6,258.22 ± 840.19 ^a
CNAD (Aa%)	13.54 ± 2.68	19.81 ± 3.21 ^a

^a *P* < 0.05

^b *P* < 0.01, versus control group

increased with the pressure, but at the same pressure, the three incremental elastic modulus of the PHT group were significantly higher than those of the control group (*P* < 0.05).

The segment incremental compliance (*C*), which was used as an indicator for the distensibility changes of hepatic portal arteries, was calculated out. As can be seen from Table 3, the compliance of the two groups decreased with the increasing of intravascular pressure; at the same

pressure the compliance of the PHT group was significantly lower than that of the control group (*P* < 0.05).

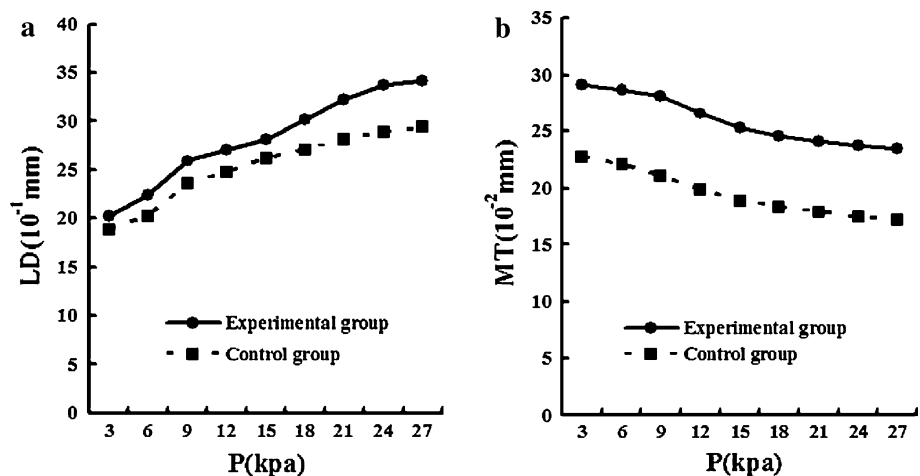
The OA of hepatic arteries is shown in Table 4. As can be seen from Table 4, with portal hypertension, the OA of the proximal and distal was significantly higher than those of the control (*P* < 0.05). Moreover, the OA of distal end was significantly higher than that of the proximal end (*P* < 0.05).

Discussion

Portal hypertension is a syndrome characterized by abnormal haemodynamical changes of portal venous system. Normally, portal veins provide the major blood supply to liver. With cirrhosis, the hepatic portal vein blood flow reduced, the maintenance of hepatic artery blood flow and the preserved HABR must be considered to protect overall hepatic circulation, so as to offset the impaired nutritive blood supply of the cirrhotic liver. Altered haemodynamics crucially deteriorates tissues and liver function and leads to the morphological and biomechanical remodelling of liver conduits of four kinds known as the portal vein system, the hepatic artery system, the hepatic vein system and the bile duct system. The significance of the biomechanical remodelling of hepatic conduits in PHT conditions is still poorly understood, even neglected. In the present study, a reliable liver cirrhosis model of swine with PHT has been established; the morphological and biomechanical remodelling of hepatic arteries has been obtained.

Our results indicate the extrahepatic vascular morphological remodelling of the hepatic arterioles in CCl₄-cirrhotic swine. The changes are reflected by the increase of luminal diameter and wall thickness, the CNND, the relative content of collagen fibers and the decrease of the relative content of elastic fiber. The results are not entirely consistent with the findings of Zipprich et al. [17] which

Fig. 2 Relationship between the lumen diameter (LD, **a**), the media thickness (MT, **b**) of hepatic artery and pressure (*P*)



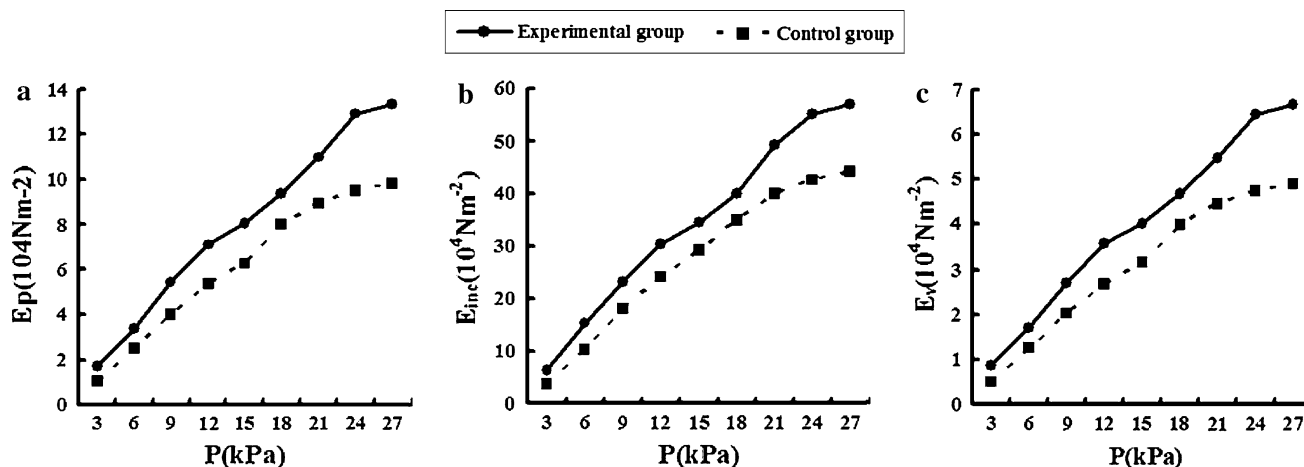


Fig. 3 Relationship between the pressure–strain elastic modulus (E_p , **a**), incremental elastic modulus (E_{inc} , **b**), volume elastic modulus (E_v , **c**), of hepatic artery and pressure (P)

Table 3 Changes of compliance of hepatic artery (Means \pm SEM, mm^2/kPa)

	Pressure				
	3	9	15	21	27
Experimental group ($n = 12$)	1.04 ± 0.04^a	0.56 ± 0.03^a	0.31 ± 0.03^a	0.21 ± 0.04^a	0.10 ± 0.02^a
Control group ($n = 6$)	1.45 ± 0.11	0.87 ± 0.07	0.57 ± 0.04	0.37 ± 0.05	0.25 ± 0.03

^a $P < 0.05$, versus control group

Table 4 Changes of opening angles of hepatic artery (Means \pm SEM, $^\circ$)

	Control group ($n = 6$)	Experimental group ($n = 12$)
Proximal segment	35.1 ± 10.2	95.8 ± 21.3^a
Distal segment	43.7 ± 13.6	$117.5 \pm 28.4^{a,b}$

^a $P < 0.05$, versus control group

^b $P < 0.05$, versus proximal segment

showed the decrease of wall thickness and the smooth muscle nuclei number of the intrahepatic vascular in CCl_4 - and BDL-cirrhotic rats. This difference might be due to the fact that the morphological changes of hepatic arteries inside and outside the liver are not consistent in cirrhosis. Since the hepatic artery is under local as well as systemic control, the two factors could influence the grade of remodelling, since during the development of portal hypertension, growth of vascular smooth muscle in vivo can be initiated by an increased load on the smooth muscle cells in the vessel wall, caused by an increased transmural pressure [24]. On the other hand, endotoxin and other toxic substances could directly injure the smooth muscle cells through the broken endothelium, the degeneration and necrosis of smooth muscle cell. The cellular nuclei of the smooth muscle cell show signs of deformation (Fig. 1a), may be it is atrophy and compensatory hyperplasia, so the

number density and area density of smooth muscle cellular nuclei increased significantly.

Blood vessel elasticity is important in physiological and pathophysiological problems involving surgery, remodelling, engineering and angioplasty. Vessel wall is a kind of visco-elastic material, characterized by creep, stress relaxation, hysteresis and so on. Young's modulus, compliance and zero-stress state (opening angle) are commonly used in describing the biomechanical properties of blood vessel. The use of a simple incremental modulus of elasticity is proposed for describing the mechanical properties of the arterial wall. The arterial wall becomes stiffer as it is extended. Compliance can be used as an indicator of blood vessel flexibility and intensity. Therefore, it has been widely used in diagnosis and prognosis assessment of cardiovascular and cerebrovascular diseases [25, 26]. Zero-stress state tension at 0 mmHg of the intact wall, a state supposedly exists when unloaded vascular rings are cut and characterized by their opening angles, can be used to reflect tissue remodelling since under zero-stress state any structural change may occur without deformation. The zero-stress state of a vessel can be the change of OA due to the non-uniform growth in the vessel wall, which reflects the changes of the residual stress [27]. Liu and Fung [28] emphasized that any mechanical analysis must begin at the zero-stress state and show axial variation along the arteries and their branches [23, 28, 29].

The results of this study also significantly indicate that with the increase of the elastic modulus of the hepatic artery, the compliance decreased in PHT group. One explanation for even more obvious increase of the hepatic arterial elastic modulus in CCl₄-cirrhosis is likely due to structural changes in the hepatic arterioles. Increases of modulus with the increasing pressure depend on the elastic properties of the collagen, elastin, and muscle within the arterial wall and their arrangement and linkages [30]. However, the elastic modulus of active muscle must be considerably greater than the tension it can exert. It is generally assumed that the collagen and elastin in the arterial wall function in parallel (Fig. 1). A parallel arrangement of the constituents implies that the properties of the arterial wall are more obviously related to radius than to pressure, which takes considerable time for a collapsed vessel to regain its original size under pressure, and significant changes in arterial elasticity are to be expected immediately after any substantial fall in blood pressure. Our results show the increase of luminal diameter and content of collagen fibres and the decrease of content of elastic fibre. So the increased elastic modulus may be associated with the increased ratio of *C* and *E*.

Data on opening angles at the zero-stress state have clinical relevance because they vary with disease, such as hypoxic hypertension [31] and diabetes [32]. Fung [27] previously suggested that the remodelling of zero-stress state was an index of the non-uniformity of growth and remodelling. Fung and Liu [31–33] showed that hypertension induced growth of intima that exceeded growth of the adventitia and then consequently induced an increase of the opening angle. Conversely, Lu et al. [34] showed that overload of flow could induce growth of adventitia that exceeded growth of the intima, thus decreasing the opening angle. Vascular reconstruction can be shown not only by the changes of the stress–strain relationship but also by the changes of zero-stress state. Zero-stress state is a specific state under physiological conditions *in vitro*. The higher the growth rate of the inner wall of blood vessels is, the larger the residual stress will be; thus the larger the OA will be induced, and vice versa. Significant increases of OA of the hepatic artery with PHT have been found in our study and bigger OA of the distal end than that of the proximal. This shows that non-uniform growth exists in the arterial wall of hepatic arteries with PHT, which may be due to the formation of false lobular liver cirrhosis and the decrease of hepatic arterial resistance in cirrhosis [17]; the tensile stress of inner arterial wall increased more quickly than that of the outer wall and hence the thickening of inner wall which is more obvious than the outer wall under the stress–growth law and the increase of OA of zero-stress state [23]. This result may be explained by the concept of a violation growth towards inside arterial wall with hypertension.

Fung and his colleagues [23, 28] showed that the opening angles of aorta at zero-stress state changed at different position from the proximal to the distal, and the structure and function of arterial wall might be different, and the OA tends to increase from the proximal to the distal. In our study, carbon tetrachloride was used to induce liver cirrhosis thus to cause PHT so as to establish the cirrhosis model of swine with PHT. The major site of resistance within the portal circulation was at the level of sinusoids, and the resistance of hepatic artery close to the liver is more obvious, so we concluded that the OA of distal end of hepatic artery with PHT was greater than that of the proximal end.

Conclusions

This study has established a reliable cirrhosis model of swine with PHT using carbon tetrachloride. Because of the serious pathological changes of liver and portal vein system, the haemodynamic changes of hepatic arteries have been prompted and thus the significant changes of mechanical remodelling of hepatic artery have taken place: the elastic modulus and the OA have been increased, while the compliance has been decreased which is a compensatory and adaptive response and in turn deteriorates the existing portal hypertension. However, which humoral factor participates in the response and how the adaptive response mechanisms take place, still need to be further explored.

Acknowledgements This study was supported by Education Department of Hubei Province Foundation (D200524002 and D20102103).

References

1. Mathie RT, Blumgart LH. The hepatic haemodynamic response to acute portal venous blood flow reductions in the dog. *Pflugers Arch* 1983;399:223–227
2. Kinoshita G, Washizu M, Motoyoshi S, Breznock EM. Effects of hypovolemic shock and reperfusion on liver blood flow in the dog. *J Vet Med Sci* 1995;57:703–708
3. Lautt WW. Relationship between hepatic blood flow and overall metabolism: the hepatic arterial buffer response. *Fed Proc* 1983;42:1662–1666
4. Lautt WW, Legare DJ, Ezzat WR. Quantitation of the hepatic arterial buffer response to graded changes in portal blood flow. *Gastroenterology* 1990;98:1024–1028
5. Ezzat WR, Lautt WW. Hepatic arterial pressure-flow autoregulation is adenosine mediated. *Am J Physiol* 1987;252:H836–845
6. Mathie RT, Alexander B. The role of adenosine in the hyperaemic response of the hepatic artery to portal vein occlusion (the 'buffer response'). *Br J Pharmacol* 1990;100:626–630
7. Mathie RT, Alexander B, Ralevic V, Burnstock G. Adenosine-induced dilatation of the rabbit hepatic arterial bed is mediated by A₂-purinoceptors. *Br J Pharmacol* 1991;103:1103–1107

8. Wang JJ, Gao GW, Gao RZ, Liu CA, Ding X, Yao ZX. Effects of tumor necrosis factor, endothelin and nitric oxide on hyperdynamic circulation of rats with acute and chronic portal hypertension. *World J Gastroenterol* 2004;10:689–693
9. Hennenberg M, Trebicka J, Biecker E, Schepke M, Sauerbruch T, Heller J. Vascular dysfunction in human and rat cirrhosis: role of receptor-desensitizing and calcium-sensitizing proteins. *Hepatology* 2007;45:495–506
10. Siebert N, Cantre D, Eipel C, Vollmar B. H2S contributes to the hepatic arterial buffer response and mediates vasorelaxation of the hepatic artery via activation of K (ATP) channels. *Am J Physiol Gastrointest Liver Physiol* 2008;295:G1266–1273
11. Tamandl D, Jorgensen P, Gundersen Y, Fuegger R, Sautner T, Aasen AO, et al. Nitric oxide administration restores the hepatic artery buffer response during porcine endotoxemia. *J Invest Surg* 2008;21:183–194
12. Bryan PT, Marshall JM. Adenosine receptor subtypes and vasodilatation in rat skeletal muscle during systemic hypoxia: a role for A1 receptors. *J Physiol* 1999;514(Pt 1):151–162
13. Richter S, Mucke I, Menger MD, Vollmar B. Impact of intrinsic blood flow regulation in cirrhosis: maintenance of hepatic arterial buffer response. *Am J Physiol Gastrointest Liver Physiol* 2000;279:G454–462
14. Fernandez-Varo G, Ros J, Morales-Ruiz M, Cejudo-Martin P, Arroyo V, Sole M, et al. Nitric oxide synthase 3-dependent vascular remodeling and circulatory dysfunction in cirrhosis. *Am J Pathol* 2003;162:1985–1993
15. Imamura M, Luo B, Limbird J, Vitello A, Oka M, Ivy DD, et al. Hypoxic pulmonary hypertension is prevented in rats with common bile duct ligation. *J Appl Physiol* 2005;98:739–747
16. Zipprich A, Mehal WZ, Ripoll C, Groszmann RJ. A distinct nitric oxide and adenosine A1 receptor dependent hepatic artery vasodilatory response in the CCl₄-cirrhotic liver. *Liver Int* 2003;3:988–994
17. Zipprich A, Loureiro-Silva MR, Jain D, D'Silva I, Groszmann RJ. Nitric oxide and vascular remodeling modulate hepatic arterial vascular resistance in the isolated perfused cirrhotic rat liver. *J Hepatol* 2008;49:739–745
18. Brandao CG, Ferreira HH, Piovesana H, Polimeno NC, Ferraz JG, de Nucci G, et al. Development of an experimental model of liver cirrhosis in rabbits. *Clin Exp Pharmacol Physiol* 2000;27:987–990
19. Van de Casteele M, Sagesser H, Zimmermann H, Reichen J. Characterisation of portal hypertension models by microspheres in anaesthetised rats: a comparison of liver flow. *Pharmacol Ther* 2001;90:35–43
20. Wang PJ, He F, Liao DH, Zhang J, Li WC, Zhang YF, et al. The impact of age on incremental elastic modulus and incremental compliance of pig hepatic portal vein for liver xenotransplantation. *Xenotransplantation* 2009;16:5–10
21. Li WC, Ruan XZ, Zhang HM, Zeng YJ. Biomechanical properties of different segments of human umbilical cord vein and its value for clinical application. *J Biomed Mater Res B Appl Biomater* 2006;76:93–97
22. Cox RH. Three-dimensional mechanics of arterial segments in vitro: methods. *J Appl Physiol* 1974;36:381–384
23. Fung YC. *Biomechanics: Mechanical Properties of Living Tissue*. 2nd edn. New York: Springer; 1993. p. 242–251
24. Seidel CL, Schildmeyer LA. Vascular smooth muscle adaptation to increased load. *Annu Rev Physiol* 1987;49:489–499
25. Fazlioglu M, Senturk T, Kumbay E, Kaderli AA, Yilmaz Y, Ozdemir B, et al. Small arterial elasticity predicts the extent of coronary artery disease: relationship with serum uric acid. *Atherosclerosis* 2009;202:200–204
26. Legedz L, Rial MO, Lantelme P, Champomier P, Cerutti C, Vincent M, et al. Markers of cardiovascular remodeling in hypertension. *Arch Mal Coeur Vaiss* 2003;96:729–733
27. Fung YC. *Biomechanics: Motion, Flow, Stress, and Growth*. New York: Springer; 1990. p. 499–533
28. Liu SQ, Fung YC. Zero-stress states of arteries. *J Biomech Eng* 1988;110:82–84
29. Liu SQ, Fung YC. Changes in the rheological properties of blood vessel tissue remodeling in the course of development of diabetes. *Biorheology* 1992;29:443–457
30. Buntin CM, Silver FH. Noninvasive assessment of mechanical properties of peripheral arteries. *Ann Biomed Eng* 1990;18:549–566
31. Fung YC, Liu SQ. Change of residual strains in arteries due to hypertrophy caused by aortic constriction. *Circ Res* 1989;65:1340–1349
32. Liu SQ, Fung YC. Influence of STZ-induced diabetes on zero-stress states of rat pulmonary and systemic arteries. *Diabetes* 1992;41:136–146
33. Liu SQ, Fung YC. Relationship between hypertension, hypertrophy, and opening angle of zero-stress state of arteries following aortic constriction. *J Biomech Eng* 1989;111:325–335
34. Lu X, Zhao JB, Wang GR, Gregersen H, Kassab GS. Remodeling of the zero-stress state of femoral arteries in response to flow overload. *Am J Physiol Heart Circ Physiol* 2001;280:H1547–1559